Exact and approximate shell geometry in the free vibration analysis of one-layered and multilayered structures

Exact and approximate shell geometry in the free vibration analysis of one-layered and multilayered structures

Salvatore Brischetto*

Abstract
The present paper proposes the study of the approximation of the curvature terms in the three-dimensional (3D) equilibrium shell equations used for the free vibration analysis of one-layered and multilayered composite and sandwich structures. 3D equilibrium equations written for spherical shells degenerate into 3D equilibrium equations for cylindrical shells and plates considering one of the two radii of curvature or both as infinite, respectively. The approximation of curvature terms has been introduced in 3D equilibrium equations in order to study its effects in terms of frequency values. This study has been conducted by means of a comparison between 3D equilibrium equation results and 3D approximate curvature equilibrium equation results. These effects depend on the thickness and curvature of the considered structure, on the embedded material and lamination sequence, on the frequency order and vibration mode. The 3D equations have been considered in exact form for simply supported structures. The system of partial differential equations has been solved by means of the exponential matrix method. A layer wise approach is considered for multilayered structures. The approximation of the curvature has been introduced in the 3D equilibrium shell equations and not in the interlaminar continuity conditions and in the top and bottom boundary and loading conditions. This choice has been made for numerical reasons. The investigation of curvature approximation effects in the equilibrium equations allows an exhaustive analysis to understand the importance of curvature terms in the free vibration problems.

Keywords: three-dimensional exact solution; shell geometry; free vibrations; vibration modes; parametric coefficients; curvature effects; curvature approximation.

1 Introduction

Shells are common structural elements in many engineering applications such as concrete roofs, exteriors of rockets, ship hulls, automobile tires, containers of liquids, oil tanks, pipes, aerospace structures and so on. A shell is defined as a curved, thin-walled structure. It can be single- or multi-layer embedding isotropic or anisotropic materials. Shells can be classified according to their curvatures. Shallow shells have rise of not more than one fifth the smallest planform dimension of the shell [1], [2]. Shells are three-dimensional (3D) bodies bounded by two relatively close, curved surfaces. In the case of shell geometries, the 3D equations of elasticity are complicated. For this reason, all shell theories reduce the 3D elasticity

*Corresponding author: Salvatore Brischetto, Department of Mechanical and Aerospace Engineering, Politecnico di Torino, corso Duca degli Abruzzi, 24, 10129 Torino, ITALY. tel: +39.011.090.6813, fax: +39.011.090.6899, e.mail: salvatore.brischetto@polito.it.

problem into a two-dimensional (2D) one for thin or thick and shallow or deep structures. This 2D simplification is usually made using Kirchhoff-Love hypotheses or their developments or refinements.

The pioneering work about the shell theory is due to Love in 1888 [3], it is considered as the first paper containing a complete and general linear theory of thin elastic shells. As discussed in the review paper by Wan and Weinitschke [4], further two important earlier publications should be considered. The first one due to Aron in 1874 [5] and the second one due to Lord Rayleigh in 1881 [6]. Aron [5] presented a set of equations for bending of thin shells to derive equations for small strains. The errors in this work were corrected by Love in his paper published in 1888 [3]. Lord Rayleigh [6] proposed a theory for the vibration of shells assuming the midsurface as unstretched. Love derived the linear equations of motion and the boundary conditions for shells, in the case of infinitesimal extensional and bending strains, using the thin plate theory assumptions by Kirchhoff [7] and the thin shell approximation conditions (e.g., as summarized in [8]). These last conditions neglect terms of the order of the thickness-to-radius of curvature ratio compared to the unit. The resulting linear shell theory was extensively used in engineering field for several decades [9] until the advent of the higher order two-dimensional shell theories that overcome some of the limitations that were intrinsic in the simplified models. The hypotheses used in the classical linear shell theories are known in the literature as Kirchhoff-Love hypotheses. The pioneering work by Love has been improved and developed in two main directions as discussed in [4]. The first direction concerns the solution techniques developed to consider different boundary and loading conditions. The second direction concerns the derivation of thin and thick shell theories from three-dimensional elasticity theory removing the Kirchhoff-Love hypotheses (e.g., asymptotic and/or iterative methods, formulation of nonlinear shell theories and their applications to finite deformation problems). One of the main problem in the development of classical and refined two-dimensional shell theories is the difficulty to understand the adequacy and accuracy of the proposed shell theory solution as approximation of the three-dimensional elasticity problem.

A number of theories exist for layered shells. Many of these theories, defined as classical ones, were developed originally for thin shells and were based on the Kirchhoff-Love kinematic hypotheses where straight lines normal to the un-deformed mid-surface remain straight and normal to the middle surface after deformation. Some of the most important classical shell theories were classified in [10]. They were named as Donnell-Mushtari, Love-Timoshenko, Arnold-Warburton, Houghton-Johns, Flügge-Byrne-Lurye, Reissner-Naghdi-Berry, Sanders, Vlasov, Kennard-Simplified and Soedel. These shell theories were also described in details in [11]. Further theories are defined as higher order ones and they overcome the main limitations connected with the simple Kirchhoff-Love hypotheses. These theories for multilayered structures can be developed in the framework of an Equivalent Single Layer (ESL) approach or a Layer Wise (LW) approach [12]. In ESL models, multilayered structures are considered as only one equivalent layer with a global stiffness that is a weighted summation of the single stiffness values of each layer. In LW models, each layer of the multilayer configuration is separately considered from the kinematic point of view.

One of the recent trends in shell analysis is the use of more rigorous shell theories, in conjunction with the numerical techniques, in order to improve the accuracy and to allow the study of various refinements in shell theories for vibration, bending and buckling analyses. As shown in [13] and [14], shells can be classified as shallow or deep (depending on the values of the curve side length of the panel-radius of curvature ratio (a/R)) and as thin or thick (depending on the value of the radius of curvature-thickness ratio (R/h) or the curve side length of the panel-thickness ratio (a/h)). Examples of thin and thick shells, and shallow and deep shells are given in Figure 1. Depending on the a/R and R/h ratios, the classical and refined 2D shell theories can give different approximation levels. For thick and/or deep shells, the use of refined 2D shell theories is mandatory. In these cases, the three-dimensional solutions could be appropriate to give correct analyses and also to propose reference solutions. However, the theory of 3D elasticity for shells is a cumbersome problem and its developing and solution procedure are usually proposed in the literature for several geometries separately (plates, circular plates, cylinders, cylindrical and spherical shells), see interesting papers [15]- [24]. These works separately analyze shell or plate geometries and they do not give a general overview for both structures. Further papers about 3D vibration analysis of shells including different boundary conditions are [25]- [27]. The exact 3D model proposed in the present paper uses a general formulation for several geometries (square and rectangular plates, open and closed cylindrical shells and spherical shell panels). The equations of motion for the dynamic case, based on the 3D elasticity theory, are written in general orthogonal curvilinear coordinates using an exact geometry for multilayered shells. The system of second order differential equations is reduced to a system of first order differential equations, and subsequently exactly solved using the exponential matrix method and the Navier-type solution. The approach is developed in a layer-wise form imposing the continuity of displacements and transverse shear/normal stresses at each interface. The exponential matrix method was already used in [28] for the three-dimensional analysis of plates in rectilinear orthogonal coordinates and in [19] for an exact, three-dimensional, free vibration analysis of angle-ply laminated cylinders in cylindrical coordinates. In the present paper, the equations of motion written in orthogonal curvilinear coordinates are a general form of the equations of motion written in rectilinear orthogonal coordinates in [28] and in cylindrical coordinates in [19]. This general exact 3D shell solution has been used by the author for the free vibration analysis of one-layered, composite, sandwich, multilayered and FGM plates, cylinders, cylindrical panels, spherical panels and carbon nanotubes [29]- [37].

In this work, the approximation of curvature terms in parametric coefficients of the 3D shell equations has been studied for thin and thick structures and for deep and shallow structures. Isotropic one-layered and orthotropic one-layered and multilayered configurations have been investigated with particular attention to the order of frequencies and the vibration modes. The introduction of a curvature approximation is a prerogative of 2D shell models. The investigation of curvature approximation effects in 3D equilibrium equations has been proposed to see when such cumbersome equations can be simplified. These curvature approximations have been introduced only in the equilibrium equations and not in interlaminar, boundary and loading condition equations in order to avoid numerical problems in the solution procedure. However, in spite of this choice, the proposed models are sufficient to give an exhaustive analysis of the importance of curvature terms in the free vibrations of shells. They allow to understand when the use of an exact shell geometry is mandatory.

2 Three-dimensional equilibrium equations

This section introduces the equilibrium equations for spherical/cylindrical shell panels and for plates. Approximation for geometry is also considered. Some of the missed equations and mathematical steps can be found in [38]- [40] where similar formulations were proposed.

2.1 Exact geometry

The three differential equations of equilibrium written for the case of free vibration analysis of multilayered spherical shells made of N_L layers with constant radii of curvature R_α and R_β are here given (the most general form for variable radii of curvature can be found in [41]- [42]):

$$H_\beta\frac{\partial\sigma^k_{\alpha\alpha}}{\partial\alpha}+H_\alpha\frac{\partial\sigma^k_{\alpha\beta}}{\partial\beta}+H_\alpha H_\beta\frac{\partial\sigma^k_{\alpha z}}{\partial z}+(\frac{2H_\beta}{R_\alpha}+\frac{H_\alpha}{R_\beta})\sigma^k_{\alpha z}=\rho^k H_\alpha H_\beta\ddot{u}^k\ , \tag{1}$$

$$H_\beta\frac{\partial\sigma^k_{\alpha\beta}}{\partial\alpha}+H_\alpha\frac{\partial\sigma^k_{\beta\beta}}{\partial\beta}+H_\alpha H_\beta\frac{\partial\sigma^k_{\beta z}}{\partial z}+(\frac{2H_\alpha}{R_\beta}+\frac{H_\beta}{R_\alpha})\sigma^k_{\beta z}=\rho^k H_\alpha H_\beta\ddot{v}^k\ , \tag{2}$$

$$H_\beta\frac{\partial\sigma^k_{\alpha z}}{\partial\alpha}+H_\alpha\frac{\partial\sigma^k_{\beta z}}{\partial\beta}+H_\alpha H_\beta\frac{\partial\sigma^k_{zz}}{\partial z}-\frac{H_\beta}{R_\alpha}\sigma^k_{\alpha\alpha}-\frac{H_\alpha}{R_\beta}\sigma^k_{\beta\beta}+(\frac{H_\beta}{R_\alpha}+\frac{H_\alpha}{R_\beta})\sigma^k_{zz}=\rho^k H_\alpha H_\beta\ddot{w}^k\ , \tag{3}$$

where ρ^k is the mass density, $(\sigma^k_{\alpha\alpha}, \sigma^k_{\beta\beta}, \sigma^k_{zz}, \sigma^k_{\beta z}, \sigma^k_{\alpha z}, \sigma^k_{\alpha\beta})$ are the six stress components and $\ddot{u}^k$, $\ddot{v}^k$ and $\ddot{w}^k$ indicate the second temporal derivative of the three displacement components. Each quantity depends on the k layer. R_α and R_β are referred to the mid-surface Ω_0 of the whole multilayered shell. H_α and H_β continuously vary through the thickness of the multilayered shell and depend on the thickness coordinate. The middle surface Ω_0 of the shell is the locus of points which lie midway between these surfaces. Geometry and the curvilinear orthogonal reference system (α, β, z) are shown in Figure 2. Displacement components are u, v, and w in α, β and z directions, respectively [43]. The parametric coefficients for shells with constant radii of curvature are:

$$H_\alpha = (1+\frac{z}{R_\alpha}) = (1+\frac{\tilde{z}-h/2}{R_\alpha}) \ , \quad H_\beta = (1+\frac{z}{R_\beta}) = (1+\frac{\tilde{z}-h/2}{R_\beta}) \ , \quad H_z = 1 \ , \tag{4}$$

H_α and H_β depend on z or $\tilde{z}$ coordinate (see Figure 3).

The strain-displacement relations of three-dimensional theory of elasticity in orthogonal curvilinear coordinates, as shown in [41] and [44], are written for the generic k layer of the multilayered spherical shell with constant radii of curvature:

$$\epsilon^k_{\alpha\alpha} = \frac{1}{H_\alpha}\frac{\partial u^k}{\partial \alpha} + \frac{w^k}{H_\alpha R_\alpha} \ , \tag{5}$$

$$\epsilon^k_{\beta\beta} = \frac{1}{H_\beta}\frac{\partial v^k}{\partial \beta} + \frac{w^k}{H_\beta R_\beta} \ , \tag{6}$$

$$\epsilon^k_{zz} = \frac{\partial w^k}{\partial z} \ , \tag{7}$$

$$\gamma^k_{\alpha\beta} = \frac{1}{H_\alpha}\frac{\partial v^k}{\partial \alpha} + \frac{1}{H_\beta}\frac{\partial u^k}{\partial \beta} \ , \tag{8}$$

$$\gamma^k_{\alpha z} = \frac{1}{H_\alpha}\frac{\partial w^k}{\partial \alpha} + \frac{\partial u^k}{\partial z} - \frac{u^k}{H_\alpha R_\alpha} \ , \tag{9}$$

$$\gamma^k_{\beta z} = \frac{1}{H_\beta}\frac{\partial w^k}{\partial \beta} + \frac{\partial v^k}{\partial z} - \frac{v^k}{H_\beta R_\beta} \ , \tag{10}$$

where symbol ∂ indicates the partial derivatives.

Eqs.(5)-(10) and constitutive equations in orthogonal curvilinear coordinates (α,β,z) for orthotropic material in the structural reference system are introduced in eqs.(1)-(3) in order to obtain the equilibrium equations written in displacement form:

$$\begin{aligned}
&(-\frac{H_\beta C^k_{55}}{H_\alpha R^2_\alpha} - \frac{C^k_{55}}{R_\alpha R_\beta})u^k + (\frac{C^k_{55}H_\beta}{R_\alpha} + \frac{C^k_{55}H_\alpha}{R_\beta})u^k_{,z} + (\frac{C^k_{11}H_\beta}{H_\alpha})u^k_{,\alpha\alpha} + (\frac{C^k_{66}H_\alpha}{H_\beta})u^k_{,\beta\beta} + (C^k_{55}H_\alpha H_\beta)u^k_{,zz} + \\
&(C^k_{12}+C^k_{66})v^k_{,\alpha\beta} + (\frac{C^k_{11}H_\beta}{H_\alpha R_\alpha} + \frac{C^k_{12}}{R_\beta} + \frac{C^k_{55}H_\beta}{H_\alpha R_\alpha} + \frac{C^k_{55}}{R_\beta})w^k_{,\alpha} + (C^k_{13}H_\beta + C^k_{55}H_\beta)w^k_{,\alpha z} = \rho^k H_\alpha H_\beta \ddot{u}^k \ ,
\end{aligned} \tag{11}$$

$$\begin{aligned}
&(-\frac{H_\alpha C^k_{44}}{H_\beta R^2_\beta} - \frac{C^k_{44}}{R_\alpha R_\beta})v^k + (\frac{C^k_{44}H_\alpha}{R_\beta} + \frac{C^k_{44}H_\beta}{R_\alpha})v^k_{,z} + (\frac{C^k_{66}H_\beta}{H_\alpha})v^k_{,\alpha\alpha} + (\frac{C^k_{22}H_\alpha}{H_\beta})v^k_{,\beta\beta} + (C^k_{44}H_\alpha H_\beta)v^k_{,zz} + \\
&(C^k_{12}+C^k_{66})u^k_{,\alpha\beta} + (\frac{C^k_{44}H_\alpha}{H_\beta R_\beta} + \frac{C^k_{44}}{R_\alpha} + \frac{C^k_{22}H_\alpha}{H_\beta R_\beta} + \frac{C^k_{12}}{R_\alpha})w^k_{,\beta} + (C^k_{44}H_\alpha + C^k_{23}H_\alpha)w^k_{,\beta z} = \rho^k H_\alpha H_\beta \ddot{v}^k \ ,
\end{aligned} \tag{12}$$

$$\begin{aligned}
&(\frac{C^k_{13}}{R_\alpha R_\beta} + \frac{C^k_{23}}{R_\alpha R_\beta} - \frac{C^k_{11}H_\beta}{H_\alpha R^2_\alpha} - \frac{2C^k_{12}}{R_\alpha R_\beta} - \frac{C^k_{22}H_\alpha}{H_\beta R^2_\beta})w^k + (-\frac{C^k_{55}H_\beta}{H_\alpha R_\alpha} + \frac{C^k_{13}}{R_\beta} - \frac{C^k_{11}H_\beta}{H_\alpha R_\alpha} - \frac{C^k_{12}}{R_\beta})u^k_{,\alpha} + \\
&(-\frac{C^k_{44}H_\alpha}{H_\beta R_\beta} + \frac{C^k_{23}}{R_\alpha} - \frac{C^k_{22}H_\alpha}{H_\beta R_\beta} - \frac{C^k_{12}}{R_\alpha})v^k_{,\beta} + (\frac{C^k_{33}H_\beta}{R_\alpha} + \frac{C^k_{33}H_\alpha}{R_\beta})w^k_{,z} + (C^k_{55}H_\beta + C^k_{13}H_\beta)u^k_{,\alpha z} + \\
&(C^k_{44}H_\alpha + C^k_{23}H_\alpha)v^k_{,\beta z} + (C^k_{55}\frac{H_\beta}{H_\alpha})w^k_{,\alpha\alpha} + (C^k_{44}\frac{H_\alpha}{H_\beta})w^k_{,\beta\beta} + (C^k_{33}H_\alpha H_\beta)w^k_{,zz} = \rho^k H_\alpha H_\beta \ddot{w}^k \ .
\end{aligned} \tag{13}$$

Coefficients C^k_{qr} are the elastic coefficients of constitutive equations for each k layer. The differential equations (11)-(13) will be solved in exact form in Section 3. The cylinder and cylindrical shell panel cases are obtained considering an infinite radius of curvature R_α (which means H_α equals 1) in equilibrium equations (1)-(3), geometrical equations (5)-(10) and displacement form of equilibrium equations (11)-(13). Plate cases are obtained considering both radii of curvature R_α and R_β as infinite (which mean H_α=H_α=1) in Eqs.(1)-(13). In the results proposed in Section 4, the 3D exact theory based on the complete equations for spherical shells will be indicated as 3D.

2.2 Approximation for geometry

In the case of thin and/or shallow shells the parametric coefficients in Eqs.(4) can be set to 1 ($H_\alpha = H_\beta = 1$) because the hypotheses $\frac{z}{R_\alpha} \simeq 0$ and $\frac{z}{R_\beta} \simeq 0$ are valid. Eqs.(1)-(3) are simplified as:

$$\frac{\partial\sigma^k_{\alpha\alpha}}{\partial\alpha} + \frac{\partial\sigma^k_{\alpha\beta}}{\partial\beta} + \frac{\partial\sigma^k_{\alpha z}}{\partial z} + (\frac{2}{R_\alpha} + \frac{1}{R_\beta})\sigma^k_{\alpha z} = \rho^k \ddot{u}^k \ , \tag{14}$$

$$\frac{\partial\sigma^k_{\alpha\beta}}{\partial\alpha} + \frac{\partial\sigma^k_{\beta\beta}}{\partial\beta} + \frac{\partial\sigma^k_{\beta z}}{\partial z} + (\frac{2}{R_\beta} + \frac{1}{R_\alpha})\sigma^k_{\beta z} = \rho^k \ddot{v}^k \ , \tag{15}$$

$$\frac{\partial\sigma^k_{\alpha z}}{\partial\alpha} + \frac{\partial\sigma^k_{\beta z}}{\partial\beta} + \frac{\partial\sigma^k_{zz}}{\partial z} - \frac{1}{R_\alpha}\sigma^k_{\alpha\alpha} - \frac{1}{R_\beta}\sigma^k_{\beta\beta} + (\frac{1}{R_\alpha} + \frac{1}{R_\beta})\sigma^k_{zz} = \rho^k \ddot{w}^k \ . \tag{16}$$

The strain-displacement relations in eqs.(5)-(10) are simplified as:

$$\epsilon^k_{\alpha\alpha} = \frac{\partial u^k}{\partial\alpha} + \frac{w^k}{R_\alpha} \ , \tag{17}$$

$$\epsilon^k_{\beta\beta} = \frac{\partial v^k}{\partial\beta} + \frac{w^k}{R_\beta} \ , \tag{18}$$

$$\epsilon^k_{zz} = \frac{\partial w^k}{\partial z} \ , \tag{19}$$

$$\gamma^k_{\alpha\beta} = \frac{\partial v^k}{\partial\alpha} + \frac{\partial u^k}{\partial\beta} \ , \tag{20}$$

$$\gamma^k_{\alpha z} = \frac{\partial w^k}{\partial\alpha} + \frac{\partial u^k}{\partial z} - \frac{u^k}{R_\alpha} \ , \tag{21}$$

$$\gamma^k_{\beta z} = \frac{\partial w^k}{\partial\beta} + \frac{\partial v^k}{\partial z} - \frac{v^k}{R_\beta} \ . \tag{22}$$

Constitutive relations do not change. The substitution of constitutive equations and eqs.(17)-(22) in equilibrium relations of eqs.(14)-(16) gives the simplified version of eqs.(11)-(13). This simplified version can directly be obtained substituting the hypotheses $H_\alpha = H_\beta = 1$ in eqs.(11)-(13):

$$(-\frac{C^k_{55}}{R^2_\alpha} - \frac{C^k_{55}}{R_\alpha R_\beta})u^k + (\frac{C^k_{55}}{R_\alpha} + \frac{C^k_{55}}{R_\beta})u^k_{,z} + (C^k_{11})u^k_{,\alpha\alpha} + (C^k_{66})u^k_{,\beta\beta} + (C^k_{55})u^k_{,zz} + (C^k_{12} + C^k_{66})v^k_{,\alpha\beta} +$$
$$(\frac{C^k_{11}}{R_\alpha} + \frac{C^k_{12}}{R_\beta} + \frac{C^k_{55}}{R_\alpha} + \frac{C^k_{55}}{R_\beta})w^k_{,\alpha} + (C^k_{13} + C^k_{55})w^k_{,\alpha z} = \rho^k \ddot{u}^k \ , \tag{23}$$

$$(-\frac{C^k_{44}}{R^2_\beta} - \frac{C^k_{44}}{R_\alpha R_\beta})v^k + (\frac{C^k_{44}}{R_\beta} + \frac{C^k_{44}}{R_\alpha})v^k_{,z} + (C^k_{66})v^k_{,\alpha\alpha} + (C^k_{22})v^k_{,\beta\beta} + (C^k_{44})v^k_{,zz} + (C^k_{12} + C^k_{66})u^k_{,\alpha\beta} +$$
$$(\frac{C^k_{44}}{R_\beta} + \frac{C^k_{44}}{R_\alpha} + \frac{C^k_{22}}{R_\beta} + \frac{C^k_{12}}{R_\alpha})w^k_{,\beta} + (C^k_{44} + C^k_{23})w^k_{,\beta z} = \rho^k \ddot{v}^k \ , \tag{24}$$

$$
\begin{aligned}
&(\frac{C^k_{13}}{R_\alpha R_\beta}+\frac{C^k_{23}}{R_\alpha R_\beta}-\frac{C^k_{11}}{R^2_\alpha}-\frac{2C^k_{12}}{R_\alpha R_\beta}-\frac{C^k_{22}}{R^2_\beta})w^k+(-\frac{C^k_{55}}{R_\alpha}+\frac{C^k_{13}}{R_\beta}-\frac{C^k_{11}}{R_\alpha}-\frac{C^k_{12}}{R_\beta})u^k_{,\alpha}+(-\frac{C^k_{44}}{R_\beta}+\frac{C^k_{23}}{R_\alpha}-\\
&\frac{C^k_{22}}{R_\beta}-\frac{C^k_{12}}{R_\alpha})v^k_{,\beta}+(\frac{C^k_{33}}{R_\alpha}+\frac{C^k_{33}}{R_\beta})w^k_{,z}+(C^k_{55}+C^k_{13})u^k_{,\alpha z}+(C^k_{44}+C^k_{23})v^k_{,\beta z}+(C^k_{55}\ )w^k_{,\alpha\alpha}+\\
&(C^k_{44}\ )w^k_{,\beta\beta}+(C^k_{33})w^k_{,zz}=\rho^k\ddot{w}^k\ .
\end{aligned}
\tag{25}
$$

The differential equations (23)-(25) will be solved in exact form in Section 3. The cylinder and cylindrical shell panel cases are obtained considering an infinite radius of curvature R_α (which means H_α equals 1) in equilibrium equations (14)-(16), geometrical equations (17)-(22) and displacement form of equilibrium equations (23)-(25). Plate cases are obtained considering both radii of curvature R_α and R_β as infinite (which mean H_α=H_α=1) in Eqs.(14)-(25). In the results proposed in Section 4, the 3D exact theory based on these equations for shells simplified by means of the hypotheses $H_\alpha = H_\beta = 1$ will be indicated as 3D($H_{\alpha,\beta}$=1).

3 Three-dimensional exact solution

The exact closed form solution for equilibrium equations detailed in Sections 2.1 and 2.2 for shells and shells with simplified geometry, respectively, will be obtained by means of the exponential matrix method and in layer-wise form. This method has been described in details in previous author's works [29]- [37] and it was also successfully applied by Messina [28] for the case of plates in rectilinear orthogonal coordinates (x,y,z) and by Soldatos and Ye [19] for the case of closed cylinders in cylindrical coordinates (ρ,θ). The equilibrium equations for shells do not have constant coefficients because of the parametric coefficients H_α and/or H_β which depend on the z coordinate. In order to obtain differential equations with constant coefficients, each k layer is divided in l mathematical layers where the parametric coefficients H_α and H_β can be easily calculated in the middle of each fictitious layer. Equilibrium equations are rewritten using $j = k\times l$ mathematical layers that allow constant coefficients to be considered (see [29] for further details).

Simply supported shells and plates are analyzed. In these cases, the three displacement components have the following harmonic form:

$$u^j(\alpha,\beta,z,t) = U^j(z)e^{i\omega t}cos(\bar{\alpha}\alpha)sin(\bar{\beta}\beta)\ , \tag{26}$$

$$v^j(\alpha,\beta,z,t) = V^j(z)e^{i\omega t}sin(\bar{\alpha}\alpha)cos(\bar{\beta}\beta)\ , \tag{27}$$

$$w^j(\alpha,\beta,z,t) = W^j(z)e^{i\omega t}sin(\bar{\alpha}\alpha)sin(\bar{\beta}\beta)\ , \tag{28}$$

where $U^j(z)$, $V^j(z)$ and $W^j(z)$ are the displacement amplitudes in α, β and z directions, respectively. i is the coefficient of the imaginary unit. $\omega = 2\pi f$ is the circular frequency where f is the frequency value, t is the time. In coefficients $\bar{\alpha} = \frac{m\pi}{a}$ and $\bar{\beta} = \frac{n\pi}{b}$, m and n are the half-wave numbers and a and b are the shell dimensions in α and β directions, respectively (calculated in the mid-surface Ω_0).

The system of second order differential equations is reduced to a system of first order differential equations in analogy with the method described in [45] and [46]. A compact form for the system of first order differential equations is:

$$\boldsymbol{D}^j\frac{\partial \boldsymbol{U}^j}{\partial \tilde{z}} = \boldsymbol{A}^j\boldsymbol{U}^j\ , \tag{29}$$

where $\frac{\partial \boldsymbol{U}^j}{\partial \tilde{z}} = \boldsymbol{U}^{j\prime}$ and $\boldsymbol{U}^j = [U^j\ V^j\ W^j\ U^{j\prime}\ V^{j\prime}\ W^{j\prime}]$. Eq.(29) can be written as:

$$\boldsymbol{D}^j\boldsymbol{U}^{j\prime} = \boldsymbol{A}^j\boldsymbol{U}^j\ , \tag{30}$$

$$\boldsymbol{U}^{j\prime} = \boldsymbol{D}^{j^{-1}}\boldsymbol{A}^j\ \boldsymbol{U}^j\ , \tag{31}$$

$$\boldsymbol{U}^{j\prime} = \boldsymbol{A}^{j*}\ \boldsymbol{U}^j\ , \tag{32}$$

with $\boldsymbol{A}^{j^*} = \boldsymbol{D}^{j^{-1}}\boldsymbol{A}^j$.

The solution of Eq.(32) can be written as (see [46]):

$$\boldsymbol{U}^j(\tilde{z}^j) = exp(\boldsymbol{A}^{j^*}\tilde{z}^j)\boldsymbol{U}^j(0) \quad \text{with} \quad \tilde{z}^j \ \epsilon \ [0, h^j] \,, \tag{33}$$

where $\tilde{z}^j$ is the thickness coordinate of each j layer from 0 at the bottom to h^j at the top (see Figure 3). The exponential matrix is calculated with $\tilde{z}^j = h^j$ for each j layer as:

$$\boldsymbol{A}^{j^{**}} = exp(\boldsymbol{A}^{j^*}h^j) = \boldsymbol{I} + \boldsymbol{A}^{j^*}h^j + \frac{\boldsymbol{A}^{j^{*2}}}{2!}h^{j^2} + \frac{\boldsymbol{A}^{j^{*3}}}{3!}h^{j^3} + \ldots + \frac{\boldsymbol{A}^{j^{*N}}}{N!}h^{j^N} \,, \tag{34}$$

where $\boldsymbol{I}$ is the 6×6 identity matrix. This expansion has a fast convergence and it is not time consuming from the computational point of view.

Considering $j = M$ mathematical layers, $M - 1$ transfer matrices must be calculated using for each interface the interlaminar continuity conditions of displacements and transverse shear/normal stresses. Moreover, the structures must be considered as simply supported and free stresses at the top and at the bottom. All these conditions allow the final system to be obtained:

$$\boldsymbol{E}\,\boldsymbol{U}^1(0) \ = \ \boldsymbol{0} \,, \tag{35}$$

where matrix $\boldsymbol{E}$ has always (6×6) dimension, independently from the number of layers M, even if the method uses a layer-wise approach. $\boldsymbol{U}^1(0)$ means $\boldsymbol{U}$ calculated at the bottom of the whole multilayered shell (first layer 1 with $\tilde{z}^1 = 0$). Further details about this procedure, and all the steps missed in this paper can be found in [29], [30] and [31] where the extensions of this 3D exact method have been made for the first time.

The free vibration analysis means to find the non-trivial solution of $\boldsymbol{U}^1(0)$ in Eq.(35) imposing the determinant of matrix $\boldsymbol{E}$ equals zero:

$$det[\boldsymbol{E}] = 0 \,, \tag{36}$$

Eq.(36) allows to calculate the roots of an higher order polynomial in $\lambda = \omega^2$. For each pair of half-wave numbers (m, n) a certain number of circular frequencies (from I to ∞) are obtained. This number depends on the order N chosen for each exponential matrix $\boldsymbol{A}^{j^{**}}$ and the number M of mathematical layers.

A certain number of circular frequencies ω_s are found when half-wave numbers m and n are imposed in the structures. For each frequency ω_s, it is possible to find the vibration mode through the thickness direction z in terms of the three displacement components u, v and w.

4 Results

Before the results proposed to analyze the curvature approximation effects in several shell geometries embedding different materials, the present 3D exact shell solution must be validated. It is important to notice that this 3D model has been successfully applied by the author for the free vibration analysis of one-layered, composite, sandwich, multilayered and FGM plates, cylinders, cylindrical panels, spherical panels and carbon nanotubes; see papers [29]- [37] for these validations and to see the choice made for the number of mathematical layers and the order of expansion for the exponential matrix.

The proposed 3D solution was successfully validated for cylindrical and spherical shell panels [29]- [37]. Several lamination sequences, thickness ratios, vibration modes and imposed half-wave numbers have been investigated. Therefore, the 3D model can be used with confidence to study the curvature approximation effects in one-layered and multilayered structures. Four different simply supported geometries are considered in the present analysis. 1) A closed cylinder with radius of curvature in α direction $R_\alpha = 10m$ and infinite radius of curvature R_β in β direction, dimensions $a = 2\pi R_\alpha$ and

$b = 20m$, and thickness ratios R_α/h equal 5, 10, 100 and 1000. 2) A cylindrical panel with radius of curvature in α direction $R_\alpha = 10m$ and infinite radius of curvature R_β in β direction, dimensions $a = \frac{\pi}{3}R_\alpha$ and $b = 20m$, and thickness ratios R_α/h equal 5, 10, 100 and 1000. 3) A spherical panel with radii of curvature in α and β directions $R = R_\alpha = R_\beta = 10m$, dimensions $a = b = \frac{\pi}{3}R$, and thickness ratios R_α/h equal 5, 10, 100 and 1000. 4) A spherical panel with in-plane dimensions $a = b = 1m$, the curve side length of the panel-radius of curvature ratio a/R_α equals 0, 0.010, 0.025, 0.050, 0.100, 0.200, 0.400, 0.500, 1.0, and the curve side length of the panel-thickness ratio a/h equals 100, 50, 20, 10 and 5. The four described geometries consider three different material configurations. 1) One-layered isotropic configuration embedding an Aluminium Alloy with Young modulus $E = 73GPa$, Poisson ratio $\nu = 0.3$ and mass density $\rho = 2800kg/m^3$. 2) A three-layered composite $90°/0°/90°$ configuration where the three layers have thickness $h/3 = h_1 = h_2 = h_3$. The composite material properties are Young modulii $E_1 = 132.38GPa$ and $E_2 = E_3 = 10.756GPa$, shear modulii $G_{12} = G_{13} = 5.6537GPa$ and $G_{23} = 3.603GPa$, Poisson ratios $\nu_{12} = \nu_{13} = 0.24$ and $\nu_{23} = 0.49$, mass density $\rho = 1600kg/m^3$. 3) A sandwich configuration with external skins made of Aluminium Alloy and thickness values $h_1 = h_3 = 0.2h$ and an internal soft core made of PVC with thickness value $h_2 = 0.6h$. The PVC properties are Young modulus $E = 0.18GPa$, Poisson ratio $\nu = 0.37$ and mass density $\rho = 50kg/m^3$. The plate cases are not investigated because no curvature approximation studies can be conducted in these cases.

Tables 1, 2 and 3 show the free frequencies for isotropic one-layered, composite three-layered and sandwich cylinders, respectively. The first six frequencies have been organized in according with the results proposed by the 2D numerical models in [34]. The first column indicates the half-wave numbers m and n imposed in α and β direction to obtain the 3D exact solution. The second column indicates the 3D frequency order (from I to ∞) for the imposed (m,n) values. The frequency results given in the third column are obtained by means of the 3D equilibrium equations for cylinders proposed in Section 2.1. The frequencies in the fourth column are calculated by means of the 3D($H_{\alpha,\beta}$=1) model of Section 2.2 obtained considering the approximation $H_\alpha = 1$ due to the hypothesis $z/R_\alpha \simeq 0$ ratio. The differences in percentage between the 3D and the 3D($H_{\alpha,\beta}$=1) models are calculated for several thickness ratios. This error is small for thin shells and it increases for thick shells. Moreover, it also depends on the considered mode: in general this error is smaller for small values of the circumferential half-wave number m. The error due to the curvature approximation also depends on the material configuration, the error is bigger for less rigid structures and/or structures with a bigger transverse anisotropy. This feature is confirmed by the fact that the biggest errors are shown for the sandwich cylinder in Table 3.

Isotropic one-layered, composite three-layered and sandwich cylindrical shell panels have been investigated in Tables 4, 5 and 6, respectively, in terms of frequency values. Each table gives the first six frequencies, for different thickness ratios, as organized in [35] by means of the 2D numerical models. The same comments and conclusions already seen for the cylinders of Tables 1, 2 and 3 are here confirmed for the cylindrical panel. The error is acceptable for thin shells and it increases for thick shells. There is a dependence on the half-wave numbers. In general, m=n=1 condition for thick shells gives the biggest errors. The sandwich configuration, which has the biggest transverse anisotropy, gives the largest errors. On the contrary, the composite configuration, which has the biggest rigidity, gives the smallest errors. In the case of in-plane vibration modes (w=0), the errors are small because the curvature effects through the thickness direction are negligible.

Tables 7, 8 and 9 show the frequency values and errors due to the curvature approximation in the free vibration analysis of isotropic one-layered, composite three-layered and sandwich spherical shell panels, respectively. Each table gives the first six frequencies organized by means of the 2D numerical models seen in [35]. All the conclusions and features seen in Tables 1-3 for cylinders and in Tables 4-6 for cylindrical shells are here confirmed for the spherical shell geometries. The only difference is due to the presence of two radii of curvature ($R_\alpha = R_\beta$) which makes more rigid the structure and allows a perfect geometrical symmetry. For these two reasons, the errors due to the curvature approximation are smaller than cylindrical (open and closed) cases. In particular, such errors are very small for thin spherical shells. It is confirmed that sandwich configurations show the biggest errors.

Tables 1-9 give an important information about the errors due to the curvature approximation when the thickness of the structure changes. Moreover, the relation between such errors and geometry, material configuration and frequency order has also been investigated. In shell structures the frequency values do not increase in a monotonic way when half-wave numbers increase because of the coupling between the three displacement components due to the curvature. In order to better understand the effects of the half-wave numbers in the errors due to the curvature approximation, the same results already seen in Tables 1-9 have been proposed in Tables 10-18 when the half-wave numbers m and n increase in a monotonic way independently by the order of frequency. For the cylinder cases of Tables 10-12 the longitudinal half-wave number n is fixed to 1 and the circumferential half-wave number m has been set to 2, 4, 6 and 8 (only even values because the cylinder is a closed structure in the α direction). In general, the error increases with the increasing of the m value. All the other features for material configuration and thickness ratio are confirmed (see Tables 1-3). The cylindrical panel cases are investigated in Tables 13-15. In these cases the values $m = 1, 2$ and $n = 1, 2$ (all the combinations) have been considered. For this geometry the relation between the errors due to the curvature approximation and the half-wave numbers m and n is not so clear as in the cylinder case. In general, the biggest error is for the couple m=1 and n=1 when the shell is thick (R_α/h equals 10 and 5) and for the couple m=2 and n=1 when the shell is thin (R_α/h equals 1000 and 100). The other comments for the material configuration and the thickness ratio are the same already seen in Tables 4-6. The spherical panel cases are investigated in Tables 16-18 for all the possible combinations of m=1,2 and n=1,2. Conclusions and comments similar to the cylindrical panel are obtained: the error is quite zero for each half-wave number combination when the shell is thin (R_α/h equals 1000 and 100). For thick spherical shells, the relation between the error due to the curvature approximation and the half-wave numbers m and n are not a priori predictable. The other comments for material configuration and thickness ratio are confirmed (see Tables 7-9).

All the results seen in Tables 1-18 show the relations between the errors due to the curvature approximation and several parameters such as thickness ratio, frequency order, half-wave numbers, geometry and material configuration. The last parameter to be considered is the curve side length of the panel-radius of curvature ratio a/R to see the effects for both shallow and deep shells. For this aim, a spherical shell panel has been investigated in Tables 19-21. Table 19 shows the isotropic one-layered spherical shell investigation when imposed half-wave numbers are m=n=1. Table 20 shows the composite three-layered spherical shell investigation when imposed half-wave numbers are m=n=1. Table 21 shows the sandwich spherical shell investigation when imposed half-wave numbers are m=n=1, m=n=2 and m=n=3, respectively. In Tables 19-21, thin and thick shells have been considered varying the curve side length of the panel-thickness ratio a/h from 100 to 5. Shallow and deep shells have been considered varying the curve side length of the panel-radius of curvature ratio a/R from 0.000 to 1.000. The errors due to the curvature approximation increases when the shell is thicker (smaller a/h values) and/or the shell is deeper (bigger a/R values). These features are general for all the material configurations and for each couple of half-wave numbers m and n. For the sandwich configuration, the (m,n) effect investigation has been added. The biggest errors are obtained for the couples m=n=2 and m=n=3.

5 Conclusions

The paper proposed the analysis of the approximation of the curvature terms in the free vibrations of one-layered and multilayered isotropic, composite and sandwich cylindrical (open and closed) and spherical shells. A three-dimensional exact solution for shell structures has been proposed in the framework of a layer-wise approach. The system of differential equations has been solved by means of the exponential matrix method. For numerical reasons, the approximation of the curvature terms has been considered only in the 3D equilibrium shell equations and not in the interlaminar continuity conditions and in the top and bottom boundary and loading conditions. However, exhaustive conclusions have been obtained. The errors in terms of frequency value due to the curvature approximation depend on the geometry, lamination and material, frequency order, vibration mode, thickness ratio and curve length of the shell-radius of curvature ratio. The curvature approximation is valid for thin and/or shallow shells. Structures including sandwich configurations usually show bigger errors because of their bigger transverse anisotropy. There is also a dependence on the half-wave numbers. For the cylinders, the error increases with the increasing of the circumferential half-wave numbers. In the cases of cylindrical and spherical shell panels, there is a dependence on the half-wave numbers but it is not a priori predictable. The error also depends on the considered vibration mode. In general, the approximation of the curvature terms does not give important errors in the case of in-plane vibration modes.

References

[1] M.S. Qatu, *Vibration of Laminated Shells and Plates*, Elsevier, Netherlands, 2004.

[2] A. Dogan and H.M. Arslan, Effects of curvature on free vibration characteristics of laminated composite cylindrical shallow shells, *Scientific Research and Essay*, 4, 226-238, 2009.

[3] A.E.H. Love, The small free vibrations and deformation of a thin elastic shell, *Philosophical Transactions of the Royal Society of London*, 179, 491-546, 1888.

[4] F.Y.M. Wan and H.J. Weinitschke, On shells of revolution with the Love-Kirchhoff hypotheses, *Journal of Engineering Mathematics*, 22, 285-334, 1988.

[5] H. Aron, Das gleichgewicht und die bewegung einer unendlich dnnen, beliebig gekrümmten elastischen schale, *Journal für die reine und angewandte Mathematik*, 78, 136-174, 1874.

[6] Lord Rayleigh, On the infinitesimal bending of surfaces of revolution, *Proceedings of the London Mathematical Society*, s1-13, 4-16, 1881.

[7] G. Kirchhoff, Über das gleichgewicht und die bewegung einer elastischen scheibe, *Journal für die reine und angewandte Mathematik*, 40, 51-88, 1850.

[8] A.J. Callegari and E.L. Reiss, Nonlinear boundary value problems for circular membranes, *Archive for Rational Mechanics and Analysis*, 31, 390-400, 1968.

[9] A.E.H. Love, *A Treatise on the Mathematical Theory of Elasticity*, Dover Publications, 4st Edition, New York, 1944.

[10] A. Farshidianfar and P. Oliazadeh, Free vibration analysis of circular cylindrical shells: comparison of different shell theories, *International Journal of Mechanics and Applications*, 2, 74-80, 2012.

[11] G.Q. Zhang, *Some Kinematic Ralations of Thin Elastic Shells*, Report LR-612, Delft Univeristy of Technology, 1989.

[12] J.N. Reddy, *Mechanics of Laminated Composite Plates and Shells: Theory and Analysis*, CRC Press, 2nd Edition, New York, 2004.

[13] E. Ventsel and T. Krauthammer, *Thin Plates and Shells: Theory, Analysis, and Applications*, Marcel Dekker, Inc., New York, 2001.

[14] F. Dau, F. Pablo and O. Polit, New reference solutions and parametric study for multilayered cylindrical shell, *International Journal of Research and Reviews in Applied Sciences*, 4, 133-161, 2010.

[15] W.-Q. Chen, H.-J. Ding and R.-Q. Xu, On exact analysis of free vibrations of embedded transversely isotropic cylindrical shells, *International Journal of Pressure Vessels and Piping*, 75, 961-966, 1998.

[16] B. Gasemzadeh, R. Azarafza, Y. Sahebi and A. Motallebi, Analysis of free vibration of cylindrical shells on the basis of three dimensional exact elasticity theory, *Indian Journal of Science and Technology*, 5, 3260-3262, 2012.

[17] N.N. Huang, Exact analysis for three-dimensional free vibrations of cross-ply cylindrical and doubly-curved laminates, *Acta Mechanica*, 108, 23-34, 1995.

[18] J.N. Sharma, D.K. Sharma and S.S. Dhaliwal, Three-dimensional free vibration analysis of a viscothermoelastic hollow sphere, *Open Journal of Acoustics*, 2, 12-24, 2012.

[19] K.P. Soldatos and J. Ye, Axisymmetric static and dynamic analysis of laminated hollow cylinders composed of monoclinic elastic layers, *Journal of Sound and Vibration*, 184, 245-259, 1995.

[20] A.E. Armenakas, D.C. Gazis and G. Herrmann, *Free Vibrations of Circular Cylindrical Shells*, Pergamon Press, Oxford, 1969.

[21] H. Zhou, W. Li, B. Lv and W.L. Li, Free vibrations of cylindrical shells with elastic-support boundary conditions, *Applied Acoustics*, 73, 751-756, 2012.

[22] S.S. Vel, Exact elasticity solution for the vibration of functionally graded anisotropic cylindrical shells, *Composite Structures*, 92, 2712-2727, 2010.

[23] C.T. Loy and K.Y. Lam, Vibration of thick cylindrical shells on the basis of three-dimensional theory of elasticity, *Journal of Sound and Vibration*, 226, 719-737, 1999.

[24] K.M. Liew, L.X. Peng and T.Y. Ng, Three-dimensional vibration analysis of spherical shell panels subjected to different boundary conditions, *International Journal of Mechanical Sciences*, 44, 2103-2117, 2002.

[25] T. Ye, G. Jin and Z. Su, Three-dimensional vibration analysis of laminated functionally graded spherical shells with general boundary conditions, *Composite Structures*, 116, 571-588, 2014.

[26] G. Jin, T. Ye and S. Shi, Three-dimensional vibration analysis of isotropic and orthotropic open shells and plates with arbitrary boundary conditions, *Shock and Vibration*, Vol. 2015, Article ID 896204, 1-29, 2015.

[27] T. Ye, G. Jin, S. Shi and X. Ma, Three-dimensional free vibration analysis of thick cylindrical shells with general end conditions and resting on elastic foundations, *International Journal of Mechanical Sciences*, 84, 120-137, 2014.

[28] A. Messina, Three dimensional free vibration analysis of cross-ply laminated plates through 2D and exact models, *3rd International Conference on Integrity, Reliability and Failure*, Porto (Portugal), 20-24 July 2009.

[29] S. Brischetto, Exact elasticity solution for natural frequencies of functionally graded simply-supported structures, *CMES: Computer Modeling in Engineering & Sciences*, 95, 391-430, 2013.

[30] S. Brischetto, Three-dimensional exact free vibration analysis of spherical, cylindrical, and flat one-layered panels, *Shock and Vibration*, Vol. 2014, Article ID 479738, 1-29, 2014.

[31] S. Brischetto, An exact 3D solution for free vibrations of multilayered cross-ply composite and sandwich plates and shells, *International Journal of Applied Mechanics*, 6, 1-42, 2014.

[32] S. Brischetto, A continuum elastic three-dimensional model for natural frequencies of single-walled carbon nanotubes, *Composites Part B: Engineering*, 61, 222-228, 2014.

[33] S. Brischetto, A continuum shell model including van der Waals interaction for free vibrations of double-walled carbon nanotubes, *CMES: Computer Modeling in Engineering & Sciences*, 104, 305-327, 2015.

[34] S. Brischetto and R. Torre, Exact 3D solutions and finite element 2D models for free vibration analysis of plates and cylinders, *Curved and Layered Structures*, 1, 59-92, 2014.

[35] F. Tornabene, S. Brischetto, N. Fantuzzi and E. Viola, Numerical and exact models for free vibration analysis of cylindrical and spherical shell panels, *Composites part B: Engineering*, 81, 231-250, 2015.

[36] S. Brischetto, F. Tornabene, N. Fantuzzi and E. Viola, 3D exact and 2D generalized differential quadrature models for free vibration analysis of functionally graded plates and cylinders, *Meccanica*, on-line, 1-40, 2016.

[37] S. Brischetto, F. Tornabene, N. Fantuzzi and M. Bacciocchi, Refined 2D and exact 3D shell models for the free vibration analysis of single- and double-walled carbon nanotubes, *Technologies*, 3, 259-284, 2015.

[38] J.R. Fan and J. Zhang, Analytical solutions for thick doubly curved laminated shells, *Journal of Engineering Mechanics*, 118, 1338-1356, 1992.

[39] W.Q. Chen and H.J. Ding, Free vibration of multi-layered spherically isotropic hollow spheres, *International Journal of Mechanical Sciences*, 43, 667-680, 2001.

[40] J.Q. Ye, *Laminated Composite Plates and Shells: 3D Modelling*, Springer, London, 2003.

[41] F.B. Hildebrand, E. Reissner and G.B. Thomas, *Notes on the Foundations of the Theory of Small Displacements of Orthotropic Shells*, NACA Technical Note No. 1833, Washington, 1949.

[42] F. Tornabene, *Meccanica delle Strutture a Guscio in Materiale Composito*, Società Editrice Esculapio, Bologna (Italy), 2012.

[43] A.W. Leissa, *Vibration of Shells*, NASA SP-288, Washington, 1973.

[44] W. Soedel, *Vibration of Shells and Plates*, Marcel Dekker, Inc., New York, 2004.

[45] G.B. Gustafson, *Systems of Differential Equations*, free available on http://www.math.utah.edu/gustafso/, accessed on 16th September 2014.

[46] W.E. Boyce and R.C. DiPrima, *Elementary Differential Equations and Boundary Value Problems*, John Wiley & Sons, Ltd., New York, 2001.

m,n	Mode	3D	3D($H_{\alpha,\beta}$=1)	Δ(%)
		R_α/h=1000		
18,1	I	3.1235	3.1359	0.40
20,1	I	3.1543	3.1695	0.48
16,1	I	3.3911	3.4002	0.27
22,1	I	3.4068	3.4238	0.50
24,1	I	3.8164	3.8345	0.47
14,1	I	4.0450	4.0508	0.14
		R_α/h=100		
10,1	I	9.5578	9.6803	1.28
12,1	I	10.413	10.576	1.56
8,1	I	11.280	11.345	0.58
14,1	I	12.848	13.029	1.41
16,1	I	16.220	16.408	1.16
6,1	I	16.676	16.700	0.14
		R_α/h=10		
6,1	I	28.721	29.968	4.34
4,1	I	30.189	30.665	1.58
8,1	I	41.416	42.942	3.68
2,1	I	49.084	49.098	0.03
2,0	I(w=0)	50.419	50.398	-0.04
6,2	I	57.691	58.615	1.60
		R_α/h=5		
4,1	I	35.847	37.226	3.85
6,1	I	47.658	50.003	4.92
2,1	I	49.918	49.956	0.08
2,0	I(w=0)	50.481	50.398	-0.16
8,1	I	74.926	77.216	3.06
4,2	I	78.468	79.720	1.59

Table 1: Simply supported isotropic one-layered cylinder. First six frequencies f in Hz (cylindrical bending frequencies have not been included) for several thickness ratios R_α/h. Error in percentage calculated as $\Delta(\%) = \frac{3D(H_{\alpha,\beta}=1)-3D}{3D} \times 100$.

m,n	Mode	3D	3D($H_{\alpha,\beta}$=1)	Δ(%)
		R_α/h=1000		
22,1	I	2.7432	2.7489	0.21
24,1	I	2.7518	2.7587	0.25
26,1	I	2.8868	2.8945	0.27
20,1	I	2.8874	2.8919	0.16
28,1	I	3.1219	3.1301	0.26
18,1	I	3.2095	3.2128	0.10
		R_α/h=100		
12,1	I	7.7168	7.7759	0.77
10,1	I	8.1510	8.1889	0.46
14,1	I	8.4061	8.4808	0.89
16,1	I	9.9229	10.006	0.84
8,1	I	9.9378	9.9566	0.19
18,1	I	12.017	12.104	0.72
		R_α/h=10		
6,1	I	20.815	21.227	1.98
4,1	I	22.378	22.484	0.47
8,1	I	26.274	26.921	2.46
2,0	I(w=0)	29.930	29.918	-0.04
2,1	I	32.637	32.616	-0.06
10,1	I	36.389	37.133	2.04
		R_α/h=5		
4,1	I	27.649	27.975	1.18
2,0	I(w=0)	29.967	29.918	-0.16
6,1	I	32.175	33.107	2.90
2,1	I	34.562	34.492	-0.20
8,1	I	45.115	46.335	2.70
0,1	I(w=0)	46.994	47.035	0.09

Table 2: Simply supported composite 90°/0°/90° cylinder. First six frequencies f in Hz (cylindrical bending frequencies have not been included) for several thickness ratios R_α/h. Error in percentage calculated as $\Delta(\%) = \frac{3D(H_{\alpha,\beta}=1)-3D}{3D} \times 100$.

m,n	Mode	3D	3D($H_{\alpha,\beta}$=1)	Δ(%)
		R_α/h=1000		
18,1	I	3.6442	3.6645	0.56
16,1	I	3.6871	3.7030	0.43
20,1	I	3.9222	3.9455	0.59
14,1	I	4.1699	4.1806	0.26
22,1	I	4.4253	4.4502	0.56
24,1	I	5.0823	5.1082	0.51
		R_α/h=100		
10,1	I	10.686	10.872	1.74
8,1	I	11.679	11.791	0.96
12,1	I	12.195	12.423	1.87
14,1	I	14.983	15.228	1.63
6,1	I	16.623	16.666	0.26
16,1	I	18.402	18.652	1.36
		R_α/h=10		
8,1	I	19.792	22.100	11.7
6,1	I	20.044	21.412	6.82
10,1	I	23.705	26.456	11.6
12,1	I	29.481	32.292	9.53
14,1	I	36.362	38.949	7.11
4,1	I	28.456	28.858	1.41
		R_α/h=5		
8,1	I	24.681	27.451	11.2
6,1	I	21.934	24.830	13.2
10,1	I	32.499	32.664	0.51
12,1	I	42.964	38.831	-9.62
14,1	I	55.277	46.088	-16.6
4,1	I	28.835	29.966	3.92

Table 3: Simply supported sandwich cylinder. First six frequencies f in Hz (cylindrical bending frequencies have not been included) for several thickness ratios R_α/h. Error in percentage calculated as $\Delta(\%) = \frac{3D(H_{\alpha,\beta}=1)-3D}{3D} \times 100$.

m,n	Mode	3D	3D($H_{\alpha,\beta}$=1)	Δ(%)
		R_α/h=1000		
3,1	I	3.1235	3.1359	0.40
4,1	I	3.8164	3.8345	0.47
2,1	I	5.2156	5.2189	0.06
5,1	I	5.6255	5.6448	0.34
4,2	I	6.4020	6.4132	0.17
5,2	I	6.6721	6.6888	0.25
		R_α/h=100		
2,1	I	10.413	10.576	1.56
1,1	I	16.676	16.700	0.14
3,1	I	20.256	20.446	0.94
2,2	I	20.342	20.439	0.48
3,2	I	23.583	23.758	0.74
3,3	I	30.344	30.494	0.49
		R_α/h=10		
1,1	I	28.721	29.968	4.34
1,2	I	57.691	58.615	1.60
0,1	I(w=0)	79.165	79.192	0.03
2,1	I	85.462	86.945	1.73
1,3	I	89.460	90.385	1.03
2,2	I	102.21	103.56	1.32
		R_α/h=5		
1,1	I	47.658	50.003	4.92
0,1	I(w=0)	79.165	79.271	0.13
1,2	I	85.354	87.045	1.98
1,3	I	134.81	136.25	1.07
2,1	I	148.53	150.09	1.05
1,0	II(w=0)	151.41	151.19	-0.14

Table 4: Simply supported isotropic one-layered cylindrical shell panel. First six frequencies f in Hz (cylindrical bending frequencies have not been included) for several thickness ratios R_α/h. Error in percentage calculated as $\Delta(\%) = \frac{3D(H_{\alpha,\beta}=1)-3D}{3D} \times 100$.

m,n	Mode	3D	3D($H_{\alpha,\beta}$=1)	Δ(%)
		R_α/h=1000		
4,1	I	2.7518	2.7587	0.25
3,1	I	3.2095	3.2128	0.10
5,1	I	3.4347	3.4432	0.25
6,1	I	4.6996	4.7086	0.19
5,2	I	5.2321	5.2378	0.11
6,2	I	5.6024	5.6101	0.14
		R_α/h=100		
2,1	I	7.7168	7.7759	0.77
3,1	I	12.017	12.104	0.72
1,1	I	13.428	13.434	0.04
3,2	I	15.595	15.663	0.44
2,2	I	15.615	15.643	0.18
4,1	I	20.620	20.711	0.44
		R_α/h=10		
1,1	I	20.815	21.227	1.98
0,1	I(w=0)	46.994	47.005	0.02
1,2	I	47.285	47.432	0.31
2,1	I	49.513	50.286	1.56
2,2	I	65.527	66.085	0.85
1,3	I	82.058	82.129	0.09
		R_α/h=5		
1,1	I	32.175	33.107	2.90
0,1	I(w=0)	46.994	47.035	0.09
1,2	I	66.117	66.499	0.58
2,1	I	83.548	84.787	1.48
1,0	II(w=0)	89.874	89.753	-0.13
0,2	I(w=0)	93.989	94.009	0.02

Table 5: Simply supported composite 90°/0°/90° cylindrical shell panel. First six frequencies f in Hz (cylindrical bending frequencies have not been included) for several thickness ratios R_α/h. Error in percentage calculated as $\Delta(\%) = \frac{3D(H_{\alpha,\beta}=1)-3D}{3D} \times 100$.

m,n	Mode	3D	3D($H_{\alpha,\beta}$=1)	Δ(%)
		R_α/h=1000		
3,1	I	3.6442	3.6645	0.56
4,1	I	5.0823	5.1082	0.51
2,1	I	5.2301	5.2364	0.12
4,2	I	7.2691	7.2880	0.26
5,1	I	7.6669	7.6936	0.35
5,2	I	8.5537	8.5783	0.29
		R_α/h=100		
2,1	I	12.195	12.423	1.87
1,1	I	16.623	16.666	0.26
2,2	I	21.415	21.560	0.68
3,1	I	22.173	22.426	1.14
3,2	I	25.159	25.392	0.93
3,3	I	31.304	31.502	0.63
		R_α/h=10		
1,1	I	20.044	21.412	6.82
2,1	I	29.481	32.292	9.54
2,2	I	37.098	39.451	6.34
1,2	I	43.940	44.668	1.66
2,3	I	49.736	51.608	3.76
3,1	I	52.796	54.181	2.62
		R_α/h=5		
1,1	I	21.934	24.830	13.2
2,1	I	42.964	38.831	-9.62
1,2	I	46.274	48.094	3.93
2,2	I	52.383	49.084	-6.30
1,3	I	66.237	67.749	2.28
2,3	I	68.193	65.776	-3.54

Table 6: Simply supported sandwich cylindrical shell panel. First six frequencies f in Hz (cylindrical bending frequencies have not been included) for several thickness ratios R_α/h. Error in percentage calculated as $\Delta(\%) = \frac{3D(H_{\alpha,\beta}=1)-3D}{3D} \times 100$.

m,n	Mode	3D	3D($H_{\alpha,\beta}$=1)	Δ(%)
		R_α/h=1000		
1,1	I	77.540	77.540	0.00
2,1	I	79.759	79.759	0.00
1,2	I	79.759	79.759	0.00
2,2	I	80.334	80.334	0.00
3,1	I	80.533	80.534	0.00
3,2	I	80.728	80.729	0.00
		R_α/h=100		
1,1	I	77.629	77.637	0.01
2,1	I	80.420	80.446	0.03
1,2	I	80.420	80.446	0.03
2,2	I	82.088	82.131	0.05
3,1	I	83.295	83.349	0.06
1,3	I	83.295	83.349	0.06
		R_α/h=10		
1,1	I	85.696	86.320	0.73
2,1	I	125.28	126.45	0.93
1,2	I	125.28	126.45	0.93
0,1	II(w=0)	150.88	151.24	0.24
1,0	II(w=0)	150.88	151.24	0.24
2,2	I	172.46	173.65	0.69
		R_α/h=5		
1,1	I	103.08	104.42	1.30
0,1	II(w=0)	149.92	151.36	0.96
1,0	II(w=0)	149.92	151.36	0.96
2,1	I	183.78	184.98	0.65
1,2	I	183.78	184.98	0.65
1,1	II(w=0)	211.97	213.94	0.93

Table 7: Simply supported isotropic one-layered spherical shell panel. First six frequencies f in Hz (cylindrical bending frequencies have not been included) for several thickness ratios R_α/h. Error in percentage calculated as $\Delta(\%) = \frac{3D(H_{\alpha,\beta}=1)-3D}{3D} \times 100$.

m,n	Mode	3D	3D($H_{\alpha,\beta}$=1)	Δ(%)
		R_α/h=1000		
1,1	I	51.297	51.297	0.00
2,2	I	54.349	54.350	0.00
3,3	I	55.064	55.064	0.00
4,4	I	55.566	55.566	0.00
3,4	I	56.333	56.334	0.00
4,5	I	56.548	56.548	0.00
		R_α/h=100		
1,1	I	51.414	51.415	0.00
2,2	I	56.685	56.693	0.01
1,2	I	61.713	61.718	0.01
3,2	I	62.283	62.300	0.03
2,3	I	66.184	66.198	0.02
3,3	I	66.361	66.379	0.03
		R_α/h=10		
1,1	I	60.003	59.987	-0.03
0,1	I(w=0)	88.903	88.759	-0.16
2,1	I	85.735	85.877	0.17
1,0	I(w=0)	89.565	89.777	0.24
1,2	I	116.12	115.91	-0.18
2,2	I	127.95	127.79	-0.12
		R_α/h=5		
1,1	I	71.499	71.159	-0.47
0,1	I(w=0)	88.990	89.816	0.93
1,0	I(w=0)	88.989	89.849	0.97
2,1	I	112.45	112.47	0.02
1,2	I	141.53	140.62	-0.64
2,2	I	164.35	163.68	-0.41

Table 8: Simply supported composite 90°/0°/90° spherical shell panel. First six frequencies f in Hz (cylindrical bending frequencies have not been included) for several thickness ratios R_α/h. Error in percentage calculated as $\Delta(\%) = \frac{3D(H_{\alpha,\beta}=1)-3D}{3D} \times 100$.

m,n	Mode	3D	3D($H_{\alpha,\beta}$=1)	Δ(%)
		R_α/h=1000		
1,1	I	76.663	76.663	0.00
2,1	I	78.863	78.864	0.00
1,2	I	78.863	78.864	0.00
2,2	I	79.443	79.444	0.00
1,3	I	79.650	79.651	0.00
3,1	I	79.650	79.651	0.00
		R_α/h=100		
1,1	I	76.815	76.830	0.02
2,1	I	79.826	79.867	0.05
1,2	I	79.826	79.867	0.05
2,2	I	81.670	81.735	0.08
3,1	I	82.884	82.961	0.09
1,3	I	82.884	82.961	0.09
		R_α/h=10		
1,1	I	78.270	78.742	0.60
2,1	I	85.061	85.974	1.07
1,2	I	85.061	85.974	1.07
2,2	I	91.834	92.600	0.83
3,1	I	96.889	97.281	0.40
1,3	I	96.889	97.281	0.40
		R_α/h=5		
1,1	I	79.023	79.688	0.84
2,1	I	91.141	87.736	-3.74
1,2	I	91.141	87.736	-3.74
2,2	I	105.65	96.675	-8.49
1,3	I	116.19	104.61	-9.97
3,1	I	116.19	104.61	-9.97

Table 9: Simply supported sandwich spherical shell panel. First six frequencies f in Hz (cylindrical bending frequencies have not been included) for several thickness ratios R_α/h. Error in percentage calculated as $\Delta(\%) = \frac{3D(H_{\alpha,\beta}=1)-3D}{3D} \times 100$.

m,n	Mode	3D	3D($H_{\alpha,\beta}$=1)	Δ(%)
		R_α/h=1000		
2,1	I	48.792	48.792	0.00
4,1	I	27.869	27.869	0.00
6,1	I	16.505	16.505	0.00
8,1	I	10.506	10.507	0.01
		R_α/h=100		
2,1	I	48.795	48.795	0.00
4,1	I	27.893	27.899	0.02
6,1	I	16.676	16.700	0.14
8,1	I	11.280	11.345	0.58
		R_α/h=10		
2,1	I	49.084	49.098	0.03
4,1	I	30.189	30.665	1.58
6,1	I	28.721	29.968	4.34
8,1	I	41.416	42.942	3.68
		R_α/h=5		
2,1	I	49.918	49.956	0.08
4,1	I	35.847	37.226	3.85
6,1	I	47.658	50.003	4.92
8,1	I	74.926	77.216	3.06

Table 10: Simply supported isotropic one-layered cylinder. First mode for m=2, 4, 6 and 8 and n=1, frequencies f in Hz for several thickness ratios R_α/h. Error in percentage calculated as $\Delta(\%) = \frac{3D(H_{\alpha,\beta}=1)-3D}{3D} \times 100$.

m,n	Mode	3D	3D($H_{\alpha,\beta}$=1)	Δ(%)
		R_α/h=1000		
2,1	I	31.764	31.764	0.00
4,1	I	19.690	19.690	0.00
6,1	I	13.326	13.326	0.00
8,1	I	9.6086	9.6088	0.00
		R_α/h=100		
2,1	I	31.773	31.773	0.00
4,1	I	19.721	19.722	0.00
6,1	I	13.428	13.434	0.04
8,1	I	9.9378	9.9566	0.19
		R_α/h=10		
2,1	I	32.637	32.616	-0.06
4,1	I	22.378	22.484	0.47
6,1	I	20.815	21.227	1.98
8,1	I	26.274	26.921	2.46
		R_α/h=5		
2,1	I	34.562	34.492	-0.20
4,1	I	27.649	27.975	1.18
6,1	I	32.175	33.107	2.90
8,1	I	45.115	46.335	2.70

Table 11: Simply supported composite 90°/0°/90° cylinder. First mode for m=2, 4, 6 and 8 and n=1, frequencies f in Hz for several thickness ratios R_α/h. Error in percentage calculated as $\Delta(\%) = \frac{3D(H_{\alpha,\beta}=1)-3D}{3D} \times 100$.

m,n	Mode	3D	3D($H_{\alpha,\beta}$=1)	Δ(%)
		R_α/h=1000		
2,1	I	48.240	48.240	0.00
4,1	I	27.554	27.554	0.00
6,1	I	16.320	16.320	0.00
8,1	I	10.395	10.397	0.02
		R_α/h=100		
2,1	I	48.245	48.245	0.00
4,1	I	27.599	27.609	0.04
6,1	I	16.623	16.666	0.26
8,1	I	11.679	11.791	0.96
		R_α/h=10		
2,1	I	48.446	48.421	-0.05
4,1	I	28.456	28.858	1.41
6,1	I	20.044	21.412	6.82
8,1	I	19.792	22.100	11.7
		R_α/h=5		
2,1	I	48.501	48.460	-0.08
4,1	I	28.835	29.966	3.92
6,1	I	21.934	24.830	13.2
8,1	I	24.681	27.451	11.2

Table 12: Simply supported sandwich cylinder. First mode for m=2, 4, 6 and 8 and n=1, frequencies f in Hz for several thickness ratios R_α/h. Error in percentage calculated as $\Delta(\%) = \frac{3D(H_{\alpha,\beta}=1)-3D}{3D} \times 100$.

m,n	Mode	3D	3D($H_{\alpha,\beta}$=1)	Δ(%)
		R_α/h=1000		
1,1	I	16.505	16.505	0.00
1,2	I	40.972	40.972	0.00
2,1	I	5.2156	5.2189	0.06
2,2	I	17.259	17.260	0.01
		R_α/h=100		
1,1	I	16.676	16.700	0.14
1,2	I	41.183	41.198	0.04
2,1	I	10.413	10.576	1.56
2,2	I	20.342	20.439	0.48
		R_α/h=10		
1,1	I	28.721	29.968	4.34
1,2	I	57.691	58.615	1.60
2,1	I	85.462	86.945	1.73
2,2	I	102.21	103.56	1.32
		R_α/h=5		
1,1	I	47.658	50.003	4.92
1,2	I	85.354	87.045	1.98
2,1	I	148.53	150.09	1.05
2,2	I	172.56	173.78	0.71

Table 13: Simply supported isotropic one-layered cylindrical shell panel. First mode for m=1,2 and n=1,2, frequencies f in Hz for several thickness ratios R_α/h. Error in percentage calculated as $\Delta(\%) = \frac{3D(H_{\alpha,\beta}=1)-3D}{3D} \times 100$.

m,n	Mode	3D	3D($H_{\alpha,\beta}$=1)	Δ(%)
		R_α/h=1000		
1,1	I	13.326	13.326	0.00
1,2	I	27.730	27.730	0.00
2,1	I	5.6341	5.6349	0.01
2,2	I	13.858	13.858	0.00
		R_α/h=100		
1,1	I	13.428	13.434	0.04
1,2	I	28.065	28.067	0.01
2,1	I	7.7168	7.7759	0.77
2,2	I	15.615	15.643	0.18
		R_α/h=10		
1,1	I	20.815	21.227	1.98
1,2	I	47.285	47.432	0.31
2,1	I	49.513	50.286	1.56
2,2	I	65.527	66.085	0.85
		R_α/h=5		
1,1	I	32.175	33.107	2.90
1,2	I	66.117	66.499	0.58
2,1	I	83.548	84.787	1.48
2,2	I	102.79	103.74	0.92

Table 14: Simply supported composite 90°/0°/90° cylindrical shell panel. First mode for m=1,2 and n=1,2, frequencies f in Hz for several thickness ratios R_α/h. Error in percentage calculated as $\Delta(\%) = \frac{3D(H_{\alpha,\beta}=1)-3D}{3D} \times 100$.

m,n	Mode	3D	3D($H_{\alpha,\beta}$=1)	Δ(%)
		R_α/h=1000		
1,1	I	16.320	16.320	0.00
1,2	I	40.511	40.511	0.00
2,1	I	5.2301	5.2364	0.12
2,2	I	17.096	17.098	0.01
		R_α/h=100		
1,1	I	16.623	16.666	0.26
1,2	I	40.869	40.895	0.06
2,1	I	12.195	12.423	1.87
2,2	I	21.415	21.560	0.68
		R_α/h=10		
1,1	I	20.044	21.412	6.82
1,2	I	43.940	44.668	1.66
2,1	I	29.481	32.292	9.53
2,2	I	37.098	39.451	6.34
		R_α/h=5		
1,1	I	21.934	24.830	13.2
1,2	I	46.274	48.094	3.93
2,1	I	42.964	38.831	-9.62
2,2	I	52.383	49.084	-6.30

Table 15: Simply supported sandwich cylindrical shell panel. First mode for m=1,2 and n=1,2, frequencies f in Hz for several thickness ratios R_α/h. Error in percentage calculated as $\Delta(\%) = \frac{3D(H_{\alpha,\beta}=1)-3D}{3D} \times 100$.

m,n	Mode	3D	3D($H_{\alpha,\beta}$=1)	Δ(%)
		R_α/h=1000		
1,1	I	77.540	77.540	0.00
1,2	I	79.759	79.759	0.00
2,1	I	79.759	79.759	0.00
2,2	I	80.334	80.334	0.00
		R_α/h=100		
1,1	I	77.629	77.637	0.01
1,2	I	80.420	80.446	0.03
2,1	I	80.420	80.446	0.03
2,2	I	82.088	82.131	0.05
		R_α/h=10		
1,1	I	85.696	86.320	0.73
1,2	I	125.28	126.45	0.93
2,1	I	125.28	126.45	0.93
2,2	I	172.46	173.65	0.69
		R_α/h=5		
1,1	I	103.08	104.42	1.30
1,2	I	183.78	184.98	0.65
2,1	I	183.78	184.98	0.65
2,2	I	259.56	260.20	0.25

Table 16: Simply supported isotropic one-layered spherical shell panel. First mode for m=1,2 and n=1,2, frequencies f in Hz for several thickness ratios R_α/h. Error in percentage calculated as $\Delta(\%) = \frac{3D(H_{\alpha,\beta}=1)-3D}{3D} \times 100$.

m,n	Mode	3D	3D($H_{\alpha,\beta}$=1)	Δ(%)
		R_α/h=1000		
1,1	I	51.297	51.297	0.00
1,2	I	60.085	60.085	0.00
2,1	I	63.690	63.690	0.00
2,2	I	54.349	54.350	0.00
		R_α/h=100		
1,1	I	51.414	51.415	0.00
1,2	I	61.713	61.718	0.01
2,1	I	64.008	64.012	0.01
2,2	I	56.685	56.693	0.01
		R_α/h=10		
1,1	I	60.003	59.987	-0.03
1,2	I	116.12	115.91	-0.18
2,1	I	85.735	85.877	0.17
2,2	I	127.95	127.79	-0.12
		R_α/h=5		
1,1	I	71.499	71.159	-0.47
1,2	I	141.53	140.62	-0.64
2,1	I	112.45	112.47	0.02
2,2	I	164.35	163.68	-0.41

Table 17: Simply supported composite 90°/0°/90° spherical shell panel. First mode for m=1,2 and n=1,2, frequencies f in Hz for several thickness ratios R_α/h. Error in percentage calculated as $\Delta(\%) = \frac{3D(H_{\alpha,\beta}=1)-3D}{3D} \times 100$.

m,n	Mode	3D	3D($H_{\alpha,\beta}$=1)	Δ(%)
		R_α/h=1000		
1,1	I	76.663	76.663	0.00
1,2	I	78.863	78.864	0.00
2,1	I	78.863	78.864	0.00
2,2	I	79.443	79.444	0.00
		R_α/h=100		
1,1	I	76.815	76.830	0.02
1,2	I	79.826	79.867	0.05
2,1	I	79.826	79.867	0.05
2,2	I	81.670	81.735	0.08
		R_α/h=10		
1,1	I	78.270	78.742	0.60
1,2	I	85.061	85.974	1.07
2,1	I	85.061	85.974	1.07
2,2	I	91.834	92.600	0.83
		R_α/h=5		
1,1	I	79.023	79.688	0.84
1,2	I	91.141	87.736	-3.74
2,1	I	91.141	87.736	-3.74
2,2	I	105.65	96.675	-8.49

Table 18: Simply supported sandwich spherical shell panel. First mode for m=1,2 and n=1,2, frequencies f in Hz for several thickness ratios R_α/h. Error in percentage calculated as $\Delta(\%) = \frac{3D(H_{\alpha,\beta}=1)-3D}{3D} \times 100$.

a/R_α	3D	3D($H_{\alpha,\beta}$=1)	$\Delta(\%)$
		a/h=100	
0.000	48.525	48.525	0.00
0.010	49.200	49.201	0.00
0.025	52.602	52.603	0.00
0.050	63.274	63.278	0.01
0.100	94.583	94.594	0.01
0.200	169.27	169.29	0.01
0.400	326.29	326.35	0.02
0.500	404.70	404.76	0.01
1.000	779.71	779.80	0.01
		a/h=50	
0.000	96.949	96.949	0.00
0.010	97.288	97.288	0.00
0.025	99.046	99.049	0.00
0.050	105.08	105.09	0.01
0.100	126.37	126.40	0.02
0.200	188.71	188.80	0.05
0.400	336.42	336.62	0.06
0.500	412.69	412.93	0.06
1.000	783.04	783.40	0.05
		a/h=20	
0.000	240.62	240.62	0.00
0.010	240.75	240.76	0.00
0.025	241.45	241.46	0.00
0.050	243.94	243.96	0.01
0.100	253.62	253.72	0.04
0.200	289.02	289.37	0.12
0.400	399.25	400.24	0.25
0.500	464.00	465.28	0.28
1.000	805.64	807.78	0.27
		a/h=10	
0.000	469.46	469.45	0.00
0.010	469.52	469.52	0.00
0.025	469.86	469.87	0.00
0.050	471.04	471.09	0.01
0.100	475.75	475.95	0.04
0.200	494.09	494.83	0.15
0.400	560.73	563.22	0.44
0.500	605.19	608.67	0.57
1.000	877.57	884.46	0.78
		a/h=5	
0.000	861.99	861.99	0.00
0.010	862.02	862.02	0.00
0.025	862.16	862.18	0.00
0.050	862.65	862.72	0.01
0.100	864.61	864.89	0.03
0.200	872.38	873.47	0.12
0.400	902.54	906.54	0.44
0.500	924.23	930.08	0.63
1.000	1080.3	1094.2	1.29

Table 19: Simply supported isotropic one-layered spherical shell panel. First mode for m=1 and n=1, frequency f in Hz. Effects of curvature a/R_α and thickness a/h. Error in percentage calculated as $\Delta(\%) = \frac{3D(H_{\alpha,\beta}=1)-3D}{3D} \times 100$.

a/R_α	3D	3D($H_{\alpha,\beta}$=1)	Δ(%)
	a/h=100		
0.000	46.893	46.893	0.00
0.010	47.219	47.219	0.00
0.025	48.893	48.893	0.00
0.050	54.451	54.451	0.00
0.100	72.520	72.523	0.00
0.200	119.94	119.94	0.00
0.400	223.80	223.81	0.00
0.500	275.76	275.77	0.00
1.000	517.77	517.78	0.00
	a/h=50		
0.000	93.380	93.380	0.00
0.010	93.543	93.543	0.00
0.025	94.392	94.393	0.00
0.050	97.364	97.365	0.00
0.100	108.42	108.43	0.01
0.200	144.25	144.27	0.01
0.400	237.12	237.16	0.02
0.500	286.32	286.37	0.02
1.000	522.08	522.13	0.01
	a/h=20		
0.000	226.75	226.75	0.00
0.010	226.81	226.81	0.00
0.025	227.14	227.14	0.00
0.050	228.33	228.33	0.00
0.100	233.00	233.01	0.00
0.200	250.73	250.78	0.02
0.400	310.54	310.69	0.05
0.500	347.64	347.83	0.05
1.000	549.53	549.70	0.03
	a/h=10		
0.000	414.54	414.54	0.00
0.010	414.57	414.57	0.00
0.025	414.72	414.72	0.00
0.050	415.27	415.27	0.00
0.100	417.45	417.47	0.00
0.200	426.04	426.08	0.01
0.400	458.13	458.27	0.03
0.500	480.17	480.34	0.03
1.000	620.53	620.37	-0.03
	a/h=5		
0.000	653.81	653.81	0.00
0.010	653.82	653.82	0.00
0.025	653.88	653.87	0.00
0.050	654.09	654.08	0.00
0.100	654.95	654.91	-0.01
0.200	658.35	658.25	-0.01
0.400	671.57	671.01	-0.08
0.500	681.09	680.21	-0.13
1.000	750.14	746.48	-0.49

Table 20: Simply supported composite 90°/0°/90° spherical shell panel. First mode for m=1 and n=1, frequency f in Hz. Effects of curvature a/R_α and thickness a/h. Error in percentage calculated as $\Delta(\%) = \frac{3D(H_{\alpha,\beta}=1)-3D}{3D} \times 100$.

		m=n=1			m=n=2			m=n=3	
a/R_α	3D	3D($H_{\alpha,\beta}$=1)	Δ(%)	3D	3D($H_{\alpha,\beta}$=1)	Δ(%)	3D	3D($H_{\alpha,\beta}$=1)	Δ(%)
				a/h=100					
0.000	62.790	62.790	0.00	214.75	214.75	0.00	402.99	402.99	0.00
0.010	63.301	63.301	0.00	214.90	214.90	0.00	403.07	403.07	0.00
0.025	65.919	65.920	0.00	215.69	215.69	0.00	403.48	403.48	0.00
0.050	74.519	74.525	0.01	218.46	218.47	0.00	404.97	404.97	0.00
0.100	101.88	101.90	0.02	229.21	229.24	0.01	410.85	410.88	0.01
0.200	172.13	172.17	0.02	267.92	268.01	0.03	433.58	433.69	0.02
0.400	325.02	325.10	0.02	385.36	385.62	0.07	514.46	514.82	0.07
0.500	402.02	402.13	0.03	453.63	453.97	0.07	567.51	568.02	0.09
1.000	771.66	771.82	0.02	821.36	822.06	0.08	892.51	893.75	0.14
				a/h=50					
0.000	107.38	107.38	0.00	301.47	301.47	0.00	509.27	509.27	0.00
0.010	107.68	107.68	0.00	301.57	301.58	0.00	509.33	509.33	0.00
0.025	109.23	109.23	0.00	302.13	302.13	0.00	509.66	509.66	0.00
0.050	114.61	114.62	0.01	304.11	304.12	0.00	510.83	510.84	0.00
0.100	133.96	134.01	0.04	311.88	311.94	0.02	515.48	515.54	0.01
0.200	192.68	192.81	0.07	341.20	341.40	0.06	533.70	533.93	0.04
0.400	335.96	336.24	0.08	439.04	439.67	0.14	600.96	601.78	0.14
0.500	410.68	411.03	0.08	499.76	500.61	0.17	646.75	647.94	0.18
1.000	775.30	775.83	0.07	846.38	848.24	0.22	943.73	946.88	0.33
				a/h=20					
0.000	161.64	161.64	0.00	387.50	387.50	0.00	669.76	669.76	0.00
0.010	161.84	161.84	0.00	387.59	387.59	0.00	669.81	669.81	0.00
0.025	162.87	162.88	0.01	388.02	388.03	0.00	670.06	670.06	0.00
0.050	166.50	166.54	0.02	389.55	389.59	0.01	670.94	670.98	0.01
0.100	180.28	180.42	0.08	395.61	395.77	0.04	674.46	674.61	0.02
0.200	227.07	227.48	0.18	418.97	419.59	0.15	688.36	688.95	0.09
0.400	356.13	357.13	0.28	501.40	503.44	0.41	741.30	743.45	0.29
0.500	426.94	428.20	0.29	555.03	557.88	0.51	778.58	781.75	0.41
1.000	782.47	784.46	0.25	878.64	885.22	0.75	1036.7	1045.7	0.87
				a/h=10					
0.000	193.75	193.75	0.00	513.21	513.21	0.00	994.85	994.85	0.00
0.010	193.92	193.92	0.00	513.27	513.27	0.00	994.88	994.87	0.00
0.025	194.77	194.79	0.01	513.59	513.60	0.00	995.04	995.01	0.00
0.050	197.80	197.89	0.04	514.74	514.77	0.01	995.62	995.50	-0.01
0.100	209.48	209.79	0.15	519.29	519.45	0.03	997.95	997.47	-0.05
0.200	250.70	251.72	0.41	537.11	537.70	0.11	1007.2	1005.3	-0.19
0.400	371.19	373.79	0.70	602.97	605.00	0.34	1043.2	1036.0	-0.69
0.500	439.32	442.61	0.75	647.81	650.68	0.44	1069.4	1058.5	-1.02
1.000	788.26	793.46	0.66	937.36	943.81	0.69	1264.6	1230.1	-2.73
				a/h=5					
0.000	256.60	256.60	0.00	823.65	823.65	0.00	1720.5	1720.5	0.00
0.010	256.73	256.73	0.00	823.69	823.66	0.00	1720.5	1720.4	-0.01
0.025	257.37	257.39	0.01	823.87	823.67	-0.02	1720.4	1719.8	-0.03
0.050	259.65	259.72	0.03	824.53	823.73	-0.10	1720.0	1717.7	-0.13
0.100	268.56	268.85	0.11	827.14	823.99	-0.38	1718.5	1710.0	-0.49
0.200	301.49	302.50	0.33	837.47	825.47	-1.43	1713.4	1686.8	-1.55
0.400	406.27	408.89	0.65	877.04	836.95	-4.57	1701.6	1638.7	-3.70
0.500	468.68	471.91	0.69	905.05	849.46	-6.14	1697.6	1619.9	-4.58
1.000	798.00	803.68	0.71	1096.7	995.44	-9.23	1712.8	1604.9	-6.30

Table 21: Simply supported sandwich spherical shell panel. First mode for several combinations of half-wave numbers (m,n), frequency f in Hz. Effects of curvature a/R_α and thickness a/h. Error in percentage calculated as $\Delta(\%) = \frac{3D(H_{\alpha,\beta}=1)-3D}{3D} \times 100$.

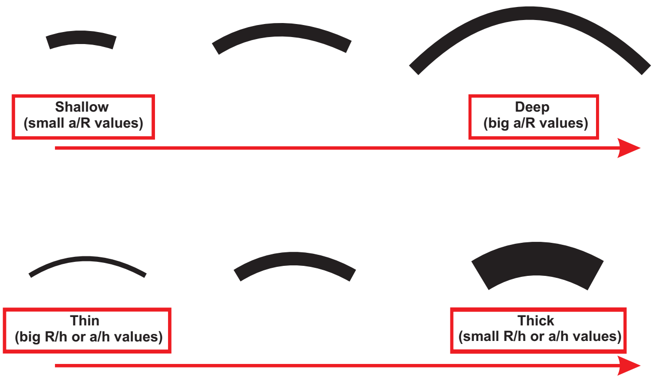

Figure 1: Shell classifications: shallow and deep shells, thin and thick shells.

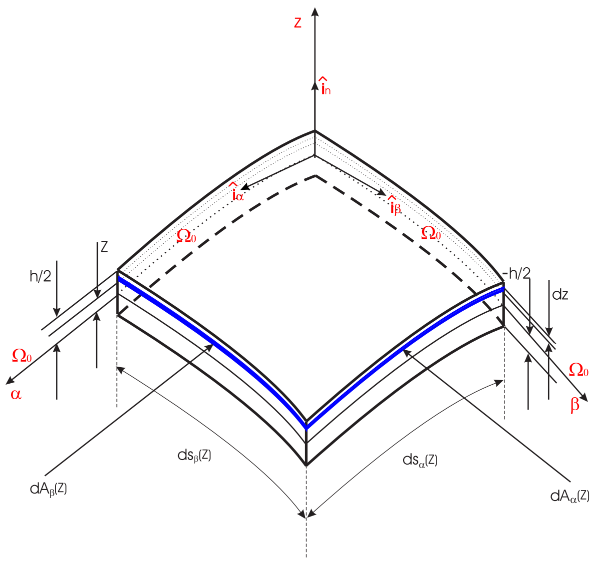

Figure 2: Reference system, geometrical parameters and notations for shells.

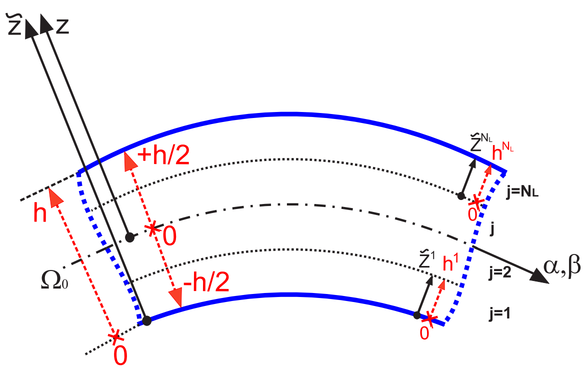

Figure 3: Reference systems and thickness coordinates z and $\tilde{z}$ for shells.